Dynamic probe of dust wakefield interactions using constrained collisions

G. A. Hebner, M. E. Riley, and B. M. Marder
Sandia National Laboratories, Albuquerque, New Mexico 87185-1423, USA
(Received 23 January 2003; published 11 July 2003)

The magnitude and the structure of the ion-wakefield potential below a negatively charged dust particle levitated in the plasma-sheath region have been determined. Attractive and repulsive components of the interaction force were extracted from a trajectory analysis of low-energy dust collisions in a well-defined electrostatic potential, which constrained the dynamics of the collisions to be one dimensional. The peak attraction was on the order of 100 fN. The structure of the ion-wakefield–induced attractive potential was significantly different from a screened-Coulomb repulsive potential.

DOI: 10.1103/PhysRevE.68.016403 PACS number(s): 52.27.Lw, 52.27.Gr

I. INTRODUCTION

Dust is a component of plasmas as diverse as interstellar regions, planetary rings, fusion reactors, and laboratory microelectronics processing systems. In these complex dusty plasmas, the plasma sheath that forms around each particle controls the interaction between the dust particles. For micron-sized dust particles immersed in idealized, isotropic plasmas, the particle interaction is well represented by a repulsive, screened Coulomb interaction. However, in most realistic systems, there is a positive ion flow around the negatively charged particles, which warps the sheath structure and generates a wakefield or a net positive space charge region downstream from the particle due to ion focusing [1–4]. Plasmas which contain negative ions can also have a warped particle-sheath structure due to negative ion flow or their accumulation at the plasma-sheath boundary layer. In addition to being of fundamental interest in gaseous electronics, Langmuir probe analysis, astronomy, and plasma theory in general, the ion wakefield has an influence on the structure of ordered, multilayer, three-dimensional (3D) plasma dust assemblies or plasma crystals. The collective interactions and the structure of such assemblies are determined by the delicate balance between the attractive and the repulsive electrostatic interactions, ion flow, and a number of other forces that typically contribute to a lesser extent. The structure of the ion wakefields that give rise to the attractive interactions is difficult to determine since their size is on the order of the plasma Debye length (50–500 μm) and the usual probe techniques are not possible. Thus the focus of this paper is on the use of the dust particles themselves to determine the magnitude and the structure of the ion-wakefield potential.

It is well known that the dust particles levitated at the plasma sheath can form single-layer (2D), hexagonal close packed, triangular lattice structures that are dominated by a repulsive screened-Coulomb (Debye) interaction [5–8]. More complicated 3D assemblies of the dusty plasmas show a range of order from face- and body-centered cubic lattices to more amorphous arrangements [9–12]. The vertical alignment of the dust particle layers is believed to be due to the ion wakefield, which gives rise to an attractive interaction. In the simplest view, the stability of the multilayer structures appears to depend on the delicate balance between an attractive ion-wakefield potential and repulsive Debye potentials [9,13]. However, this simple view is not universally accepted since the largest 3D dust arrangements apparently show little wakefield effect [14]. Melzer and co-workers recently observed a nonreciprocal attractive interaction between the two different mass particles [15,16]. They measured an attractive force of the order of 1–8 fN for a He plasma and dust particles considerably smaller than those used here. Their technique used a laser to push the particles a small distance away from the minimum of the attractive potential well. From an analysis of the particle trajectories after the laser is turned off and the particles relax back to an equilibrium position, a portion of the attractive potential well can be determined. Our technique determines the shape of the entire potential well since it examines the constrained 1D collisions between the particles that originate at far distances from each other.

II. RESULTS AND DISCUSSION

A. Calculation of the shape of the wakefield structure

In order to gain an understanding of the wakefield potential structure, we performed a self-consistent, azimuthally symmetric calculation of plasma shielding about a dust particle. It is a feature of our work that we are investigating the forces *independent* of any model of the interaction. This model only serves as a guide to understand the approximate shape and potential in these systems. We integrated the collisionless Newtonian equations of motion (NEOM) for ions flowing past a particle of fixed charge, computed the space charge density from the ion trajectories and a Boltzmann distribution of the electrons, and solved the Poisson equation for the new field. This procedure was iterated to steady state and is shown in Fig. 1. Thus the solution includes a self-consistent space charge. In general, the simulation captures the downstream potential formed by ion focusing observed in previous simulations of this problem, each with their own simplifying assumptions [1,17–19]. The trajectories for small impact parameters focus on the axis creating a region of increased positive space charge below the particle. The ''bounce'' of ions at $r=0$ was due to cylindrical symmetry. The ion-neutral mean free path (including charge exchange) is estimated to be of the order of 0.5 mm at 100 mTorr, comparable to our observed interparticle spacing of 0.3–0.8 mm. This indicates that a collisionless solution of the self-

 ©2003 The American Physical Society

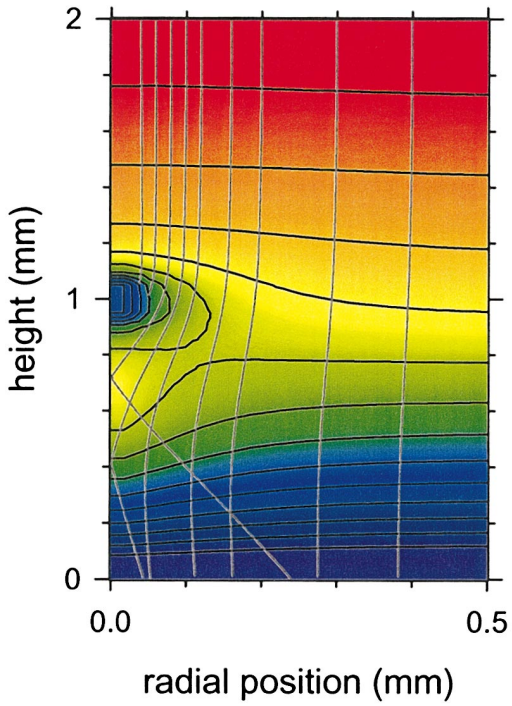

FIG. 1. (Color) Representative, azimuthally symmetric, self-consistent solution of potential and ion trajectories around a charged sphere in the plasma-presheath region. The horizontal lines are equipotentials spaced by 0.05 V, while the vertical lines are selected trajectories of argon ions moving from top to bottom. Particle surface charge was 35 000 electrons, particle diameter was 8 μm, electron temperature was 1 eV, and incident ion energy was 0.5 eV.

consistent space charge problem is approximately correct. However, a full solution of the problem that includes both collisions and a self-consistent space charge is beyond the scope of this effort.

A saddle point is formed in the potential due to the combination of the electrode-sheath potential and the sheath about the particle. For these plasma conditions, which are in the range of our typical experimental values, the minimum of the potential well was 0.3 mm below the particle and was 0.1 V deep. The electrostatic force on a second test particle colliding with this particle and its associated ion wakefield would depend on the vertical offset between the particles. If the test particle was at the same height, it would essentially interact with a repulsive potential. If the test particle had a larger diameter (and thus has a equilibrium height below the particle), its interaction is a complicated combination of repulsive interactions between the two particles and an attractive interaction between the test particle and the ion wake field. In addition to the electrostatic interaction, Lapenta indicates that the focused ion wind produces a stronger force than the electrostatic force in a dusty plasma similar to our system [20]. However, our estimates of the ion wind force do not indicate that it is quite so dominant, a difference that must be resolved in future studies.

B. Experimental setup

We derive the wakefield potential associated with an upper target dust particle by colliding it with a probe dust particle levitated at a lower height. A sketch of the particle interactions and distance definitions is shown in Fig. 2, while a top view of the experimental configuration is shown in Fig. 3. For this work, the 0.5 m radius of curvature lower electrode insert used in previous work on plasma dust layer compression [5,6] was modified to include a shallow trench. The trench formed an electrostatic trough in the plasma which confined the particles to 1D motion with a radially dependent damped velocity. With this arrangement, we could reproducibly generate head-on collisions with a constant vertical offset (impact parameter). The vertical confining forces (electric sheath, gravity, and ion wind) [6] are much stronger than the weak particle-particle interactions or random Brownian motion, resulting in *collision dynamics constrained to motion in the coordinate axis parallel to the trough*. The vertical movement of the injected particles damped quickly, as did any oscillation normal to the trough. In addition, the amplitude of Brownian motion normal to the trough was considerably less than the particle's distance of closest approach.

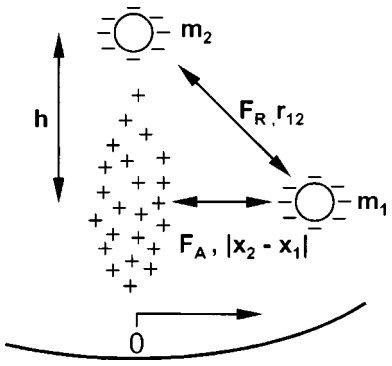

FIG. 2. Schematic of two particles showing upper particle of mass m_2, lower particle of mass m_1, and ion wakefield (positive space charge region) below the upper particle. The 0.5 m radius of curvature of the lower electrode is greatly exaggerated.

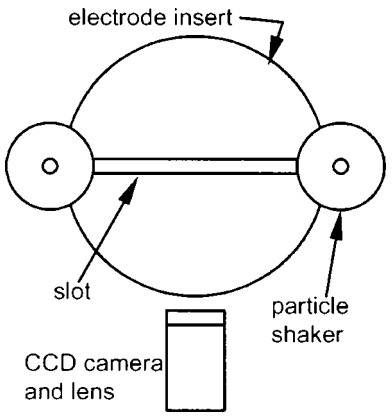

FIG. 3. Top view of the experimental configuration. The 51-mm-diameter electrode insert has a shallow 0.5 m radius of curvature cut into the top surface. The slot is 3 mm wide and 2 mm deep and follows the 0.5 m curvature. Two-particle shakers are located at either end of the trench and are lightly tapped to drop single particles into the electrostatic trough formed by the plasma above the slot.

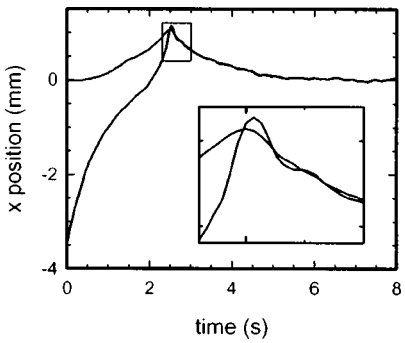

FIG. 4. Horizontal (x) coordinates of the 8.34- and 11.93-μm-diameter particles as a function of time. The 8.34-μm-diameter particle (upper) is located at the center of the well ($x=0$ mm) at $t=0$. The inset is an expanded view of the oscillatory particle motion within the box ($t=2.3-3.0$ s and x position$=0.4-1.2$ mm).

For most of the experiments discussed, a single Melamine particle with a diameter of 8.34 ± 0.11 μm was dropped into one end of the trough and fell to the bottom of the spherical electrode with an exponential time constant determined by the gas drag [5,6]. At a later time, a second particle with a diameter of 11.93 ± 0.21 μm was dropped into the opposite end of the trough. The resulting interaction as the particles collided at the bottom of the well was then recorded and analyzed. The particles were illuminated using a sheet of light produced by a 532-nm, 10-mW laser, scanning mirror, and cylindrical lens. Top and side views of the time dependent trajectories were captured on a videotape using two charge coupled device cameras and lenses. The videotape was digitized frame by frame, and the particle's position was extracted using image analysis algorithms. The time spacing was 30 frames/s. The experiments were performed in an asymmetrically driven, parallel plate discharge chamber, a modified gaseous electronics conference rf reference cell [21]. The lower electrode was capacitively coupled and driven at 20 MHz and 1.8 W [6]. Argon gas flow was 2 SCCM at 100 mTorr. The particle charge and the screening length were determined from a separate analysis of the compression of the 1D line of particles in the parabolic well, and were not derived from these collision studies. That analysis, which is not critical to this work and will be published elsewhere, was an extension of our derivation of Z and λ from an analysis of the compression of 2D dusty plasma assemblies of various sizes [5,6]. The charge on the dust particles were 7400, 10 400, 14 300, and 19 500 electrons, and the screening length was 270, 330, 410, and 400 μm for particle diameters of 6.86, 8.34, 9.78, and 11.93 μm, respectively

C. Experimental derivation of the attractive and repulsive potentials

An example of the time dependent trajectories is shown in Fig. 4. Only the horizontal distance between the particles is shown or analyzed. The vertical position between the particles of 0.62 mm, varied by less than 0.02 mm, reflecting the strong vertical confining forces and the lack of changes in the particle charge. At $t=0$, the upper (8.34 μm) target particle was at the bottom of the gravitational potential well formed by the curved electrode. The lower (11.93 μm) probe particle was moving towards the center of the well due to gravity, with a position (velocity) that had the previously observed exponential dependence due to the gas drag [5,6]. At a horizontal spacing of less than 2 mm ($t>0.5$ s), the upper particle begins to move away from the lowest point of the gravity well, gaining potential energy. This motion shows that the upper particle was responding to a repulsive pairwise interaction. At the same time, the lower particle moves with the upper particle up the potential energy well formed by the curved lower electrode. The lower particle was both attracted to the ion wakefield below the upper particle and, by reciprocity, repelled by the negative charge. As the upper particle moved away from the minimum of the gravitational well in response to the repulsive interactions between the particles, the lower particle was attracted to the ion wakefield, further driving the upper particle away from the center. For this time period, it appears that the attractive interaction is stronger than the repulsive interaction. At $t\approx2.5$ s, the repulsive force was no longer adequate to push the upper particle up the radially increasing gravitational potential well, and the lower particle fell into the ion wakefield. The lower particle oscillated a couple of times when it fell into the bottom of the wakefield potential well, although at this pressure the oscillation amplitude was small. With the horizontal component of the repulsive force on the upper particle removed because of the near-vertical orientation, the particles drifted back to the center of the gravitational potential well as a pair with an exponential time constant dominated by the gas drag on the *upper* particle.

The interaction potentials are obtained from the particles' position and velocity by numerically inverting the NEOM shown below. Due to the experimental geometry and the vertically constrained motion, we have only a 1D set of equations. The upper particle interacts with the lower particle through a repulsive potential given by a Debye interaction $V_D(r_{12})=D/r_{12}\exp(-r_{12}/\lambda_D)$, where λ_D is the screening length; $D=q_1q_2/4\pi\varepsilon_0$, with q_i the charge on particle i; and $r_{12}=\sqrt{(x_1-x_2)^2+h^2}$, with h the vertical spacing between the particles and x_i the coordinate parallel to the trough. The lower particle, however, responds to both the above repulsive interaction and an attractive force generated between it and the wakefield, $V_A(|x_1-x_2|,h)$. In this limit, the NEOM for the two particles are

$$m_1\ddot{x}_1+m_1\gamma_1\dot{x}_1+k_1x_1=\left(\frac{x_2-x_1}{r_{12}}V_D'-\frac{\partial}{\partial x_1}V_A(|x_1-x_2|,h)\right), \tag{1}$$

$$m_2\ddot{x}_2+m_2\gamma_2\dot{x}_2+k_2x_2=\frac{x_1-x_2}{r_{12}}V_D'(r_{12}), \tag{2}$$

where m_i is the mass; γ_i is the Epstein drag coefficient; and $k_i=m_ig/R_c$, with g the acceleration due to gravity and R_c the radius of curvature of the electrode. Rather than calculate the Epstein drag coefficients, we experimentally determine the values for each experimental condition, since we find that the value of the attractive force, which should be zero for large particle separations, depended strongly on the value of

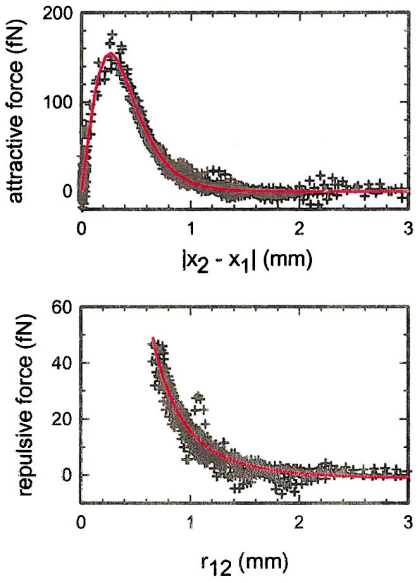

FIG. 5. (Color) The attractive and repulsive forces derived from analysis of eight collisions. The solid red lines are fits to the attractive potential [Eq. (3)] and repulsive screened-Coulomb form. The fit parameters for the attractive interaction energy were $A/\lambda = -397\times10^{-14}$ N, $a=410$ μm, and $\lambda=185$ μm. For the repulsive interaction, $D=2.7\times10^{-20}$ Jm and $\lambda_D=750$ μm.

the gas drag. As in the previous work, the measured drag coefficients are in good agreement with the calculated values [6]. We then solve for the attractive force $F_A=-(\partial/\partial x)V_A(|x_1-x_2|,h)$ and the repulsive force $F_R=V_D'(r_{12})$ as functions of the interparticle spacing. While the lower particle also has an ion wakefield associated with it, the dipole interaction between the lower particle wake field and the upper particle is small due to the distance, and is thus neglected in this analysis. We note that our technique of directly inverting the NEOM avoids (within measurement accuracy) specifying the functional forms of the particle-particle interaction. Because we know the confining force due to the curved electrode, the drag force due to neutral gas scattering, and the charges of the particles by single-layer analysis [5] we can isolate the full interaction of the particles.

The particle positions as functions of time, were inserted into Eqs. (1) and (2) to directly determine the attractive and repulsive potentials from the trajectory data. The first and second derivatives (velocity and acceleration) were calculated after three-point smoothing was performed on the data. Experimentally measured Epstein gas-damping rates of 25 and 17.5 s^{-1} were used for the 8.34- and 11.93-μm-diameter particles, respectively [5]. Experimentally determined attractive and repulsive forces are shown in Fig. 5 as points. The data from eight independent collision events are shown. The peak attractive force is approximately 160 fN, while the peak repulsive force is 50 fN. Whether an upper particle was injected towards the already present lower particle or visa versa made no difference since the eight collision events shown have four of each particle addition order. We note that our peak attractive force is more than an order of magnitude larger than the previous measurements [15,16]. This difference is likely due to variations in particle charge and size, gas, and plasma conditions, all of which suggest additional work.

D. Derivation of the functional form of the attractive potential

To find a functional form of the wakefield potential, we used an approximate thermal average of the first-order result for ion scattering from a Debye interaction of screening length λ_D. The analysis shows that the dominant cylindrical radial dependence of the wakefield potential is expected to be of the form

$$V(r)=A\exp(-\sqrt{a^2+r^2}/\lambda), \tag{3}$$

where A is a function of plasma and dust parameters, and a depends on the thermal averaging of ion motion.

Fits to the experimental data are shown as lines on Fig. 5. The usefulness of Eq. (3) lies in the fit to the experimental data; the approximations made in the derivation are too many to be universally useful as a predictive result. From the regression fits, we calculate that the wakefield potential well, if electrostatic, is about 0.2 V deep at the separation of the two particles of 0.6 mm, in reasonable agreement with our calculations (Fig. 1). The fit to the repulsive force yields a D value that is consistent with our measured particle charge, but a screening length that is approximately a factor of 2 larger than that derived from the analysis of the particle monolayer compression [6]. The larger value of the screening length is approaching the electron Debye length. We hypothesize that this is due to the higher ion velocity in the vicinity of the particles, giving less ion screening and a larger Debye length.

E. Variation of vertical particle separation

In principle, the vertical structure of the ion-wakefield potential can be measured by varying the vertical separation between the two particles. We have begun to scope out this interaction using the limited range of particles we currently have. For 6.86-μm-diameter particles, only repulsive interactions were observed [5,6]. For 6.86- and 8.34-μm-diameter particles, $h=0.13$ mm and only repulsive interactions were observed. For 6.86- and 9.78-μm-diameter particles ($h=0.52$ mm), a weak attractive potential was observed (Fig. 6). However, unlike the data in Fig. 4, the particles never align vertically. The attractive interaction was not strong enough to overcome the repulsive interaction and drive the lower particle completely into the ion-wakefield potential. Rather, the particles went to an unaligned position *away from the minimum* of the gravitational potential well. Particle molecular dynamic (MD) simulations also display this phenomenon using the experimentally determined interactions. Those models suggest that the off-center orientation occurs because the ion flow to the electrode is asymmetrically deflected by the pair of particles, creating a horizontal component of force. This off-center arrangement was also noted in the previous work and also was shown to depend on pressure which modified the particle charge and the characteristics of the positive space charge ion-wakefield potential [16].

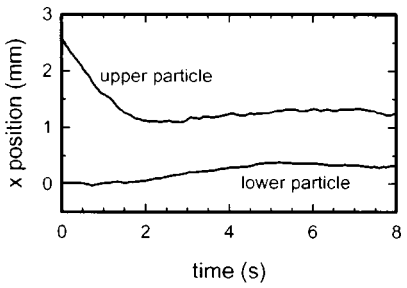

FIG. 6. Time dependent horizontal position of 6.86- and 9.78-μm-diameter particles. In this case the 9.78-μm-diameter particle was located at $x=0$ for $t=0$. In this case, the particles were held apart by the repulsion, and the lower particle did not enter the wakefield potential well.

Using the experimentally determined potential interactions and our MD simulations of particle motion, we also predict *stable oscillatory states* of vertical particle pairs for particle pair parameters close to the present conditions (particle charges of 5500 and 21 600 electrons, $h=0.6$ mm). The two particles remain nearly vertical, and oscillate horizontally *in phase* at 2–3 Hz about a common vertical line with the lower particle having larger amplitude, 0.8 mm vs 0.5 mm. We have yet to experimentally observe this oscillation, likely because we have not generated the right combination of particle charge and spacing.

III. SUMMARY

In summary, the magnitude and the structure of the ion-wakefield potential formed by a single particle immersed in a plasma were determined from the low-energy constrained collisions between the target and the probe particle. In addition to addressing the fundamental questions of ion flow effects on the structure of the dust plasma sheath, it now seems clear that the number of the instabilities observed, when 3D arrangements are attempted, are due to the characteristics of the attractive potential. These measurements of the absolute forces on the particle will be of use in molecular dynamic simulations of multilayer assemblies to define regions of stability for the formation of 3D dust particle plasma assemblies.

ACKNOWLEDGMENTS

This work was supported by the Division of Material Sciences, BES, Office of Science, U.S. Department of Energy, and Sandia National Laboratories, a multiprogram laboratory operated by Sandia Corporation, a Lockheed Martin Company for the U.S. Department of Energy's National Nuclear Security Administration under Contract No. DE-AC04-94AL85000.

[1] V. A. Schweigert *et al.*, Phys. Rev. E **54**, 4155 (1996).
[2] A. Melzer, V. A. Schweigert, and A. Piel, Phys. Rev. E **54**, R46 (1996).
[3] V. N. Tsytovich, Phys. Usp. **40**, 53 (1997).
[4] M. Lampe *et al.*, Phys. Plasmas **7**, 3851 (2000).
[5] G. A. Hebner *et al.*, Phys. Rev. Lett. **87**, 235001 (2001).
[6] G. A. Hebner, M. E. Riley, and K. E. Greenberg, Phys. Rev. E **66**, 046407 (2002).
[7] G. A. Hebner *et al.*, IEEE Trans. Plasma Sci. **30**, 94 (2002).
[8] U. Konopka, G. E. Morfill, and L. Ratke, Phys. Rev. Lett. **84**, 891 (2000).
[9] K. Takahashi *et al.*, Phys. Rev. E **58**, 7805 (1998).
[10] J. B. Piper, J. Goree, and R. A. Quinn, Phys. Rev. E **54**, 5636 (1996).
[11] Y. Hayashi, Phys. Rev. Lett. **83**, 4764 (1999).
[12] G. E. Morfill *et al.*, Phys. Rev. Lett. **83**, 1598 (1999).
[13] V. Steinberg *et al.*, Phys. Rev. Lett. **86**, 4540 (2001).
[14] M. Zuzic *et al.*, Phys. Rev. Lett. **85**, 4064 (2000).
[15] A. Melzer, V. A. Schweigert, and A. Piel, Phys. Rev. Lett. **83**, 3194 (1999).
[16] A. Melzer, V. A. Schweigert, and A. Piel, Phys. Scr. **61**, 494 (2000).
[17] F. Melandso and J. Goree, Phys. Rev. E **52**, 5312 (1995).
[18] M. Lampe, G. Joyce, G. Ganguli, and V. Gavrishchaka, Phys. Plasmas **7**, 3851 (2000).
[19] S. V. Vladimirov, S. A. Maiorov, and N. F. Cramer, Phys. Rev. E **67**, 016407 (2003).
[20] G. Lapenta, Phys. Rev. E **66**, 026409 (2002).
[21] P. J. Hargis, Jr. *et al.*, Rev. Sci. Instrum. **65**, 140 (1994).